Heat Transfer Augmentation due to Surface Roughness: Ballistic Range Tests of Saturn and Uranus Atmospheric Entry Probes

Michael Wilder, Dinesh Prabhu*, and Daniel Reda
Aerothermodynamics Branch
NASA-Ames Research Center
and
* ERC, Inc.,
Moffett Field, CA

The 10th International Planetary Probe Workshop
San Jose, CA, 17-21 June, 2013

This research was funded by Planetary Science Division of the NASA Science Mission Directorate.

Abstract

- **Experiments are underway in the NASA Ames hypersonic ballistic range to measure the effects of surface roughness on turbulent convective heat transfer to spherically-blunted large-angle cones.**

- **Initial results presented here quantify the turbulent heat-transfer augmentation due to surface micro-roughness:**
  - Micro-roughness patterns form under laminar-flow ablation conditions early in the entry (high altitude, low Reynolds number)
  - Roughness interacts with the surface shear layer to increase heat transfer and shear

Composite of Two Flights: M = 8.5

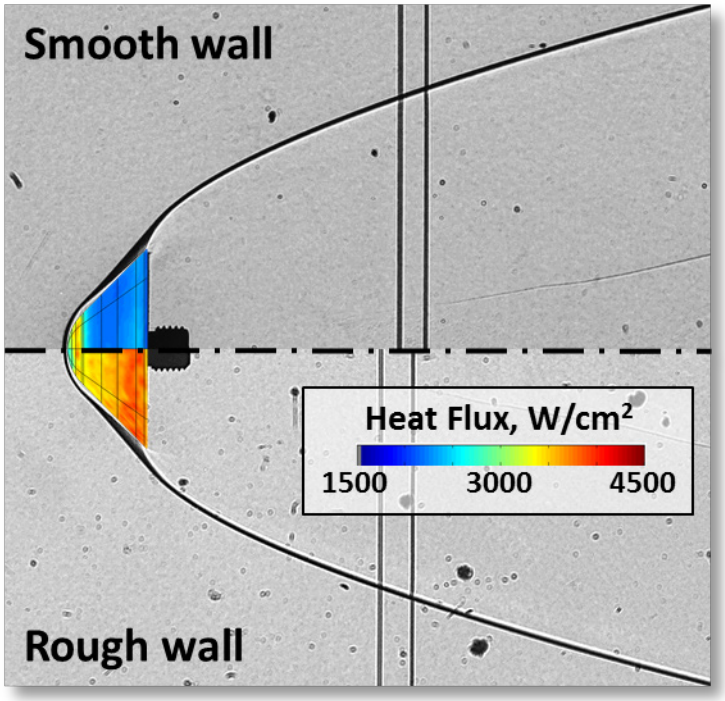

Outline

- Statement of the Problem
- Objectives of the Experiments
- Experimental Approach
- Results
- Summary
- Future Work

Statement of the Problem

- **Probes to outer planets (and Venus) will require ablative thermal protection systems (TPS) to survive extreme heating environments**
- **Ablation of TPS materials under laminar-flow (high-altitude, low-pressure) conditions results in surface micro-roughness characteristic of the material**

Example Micro-roughness of Ablated Chop-Molded Carbon Phenolic

Ablated in the Ames IHF Arcjet
courtesy: M. Stackpoole, NASA Ames

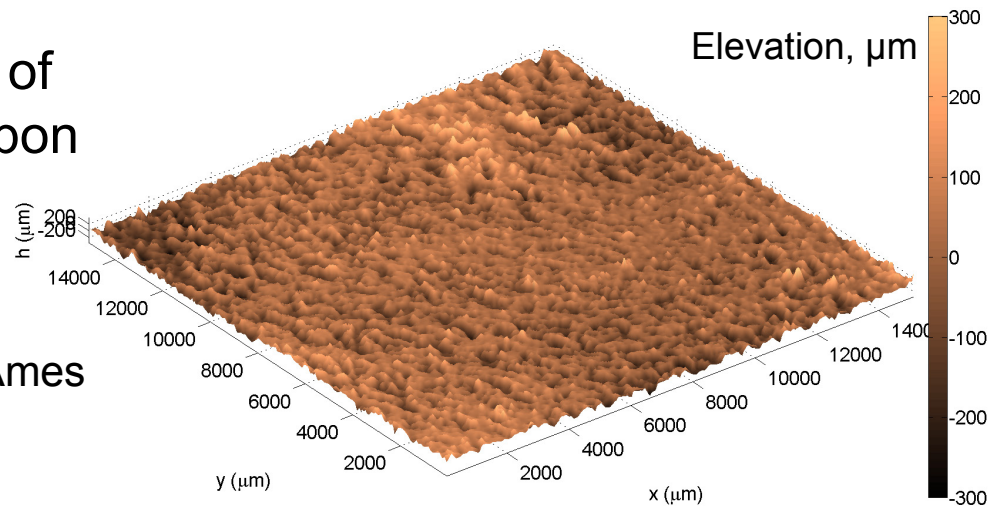

Statement of the Problem

- **Surface micro-roughness can increase aerodynamic heating (and ablation rates) by**
  - inducing transition to turbulent flow
  - enhancing turbulent heating
- **Turbulent heat transfer augmentation**
  - is a boundary layer flow phenomenon
  - requires roughness sizes taller than the viscous sublayer

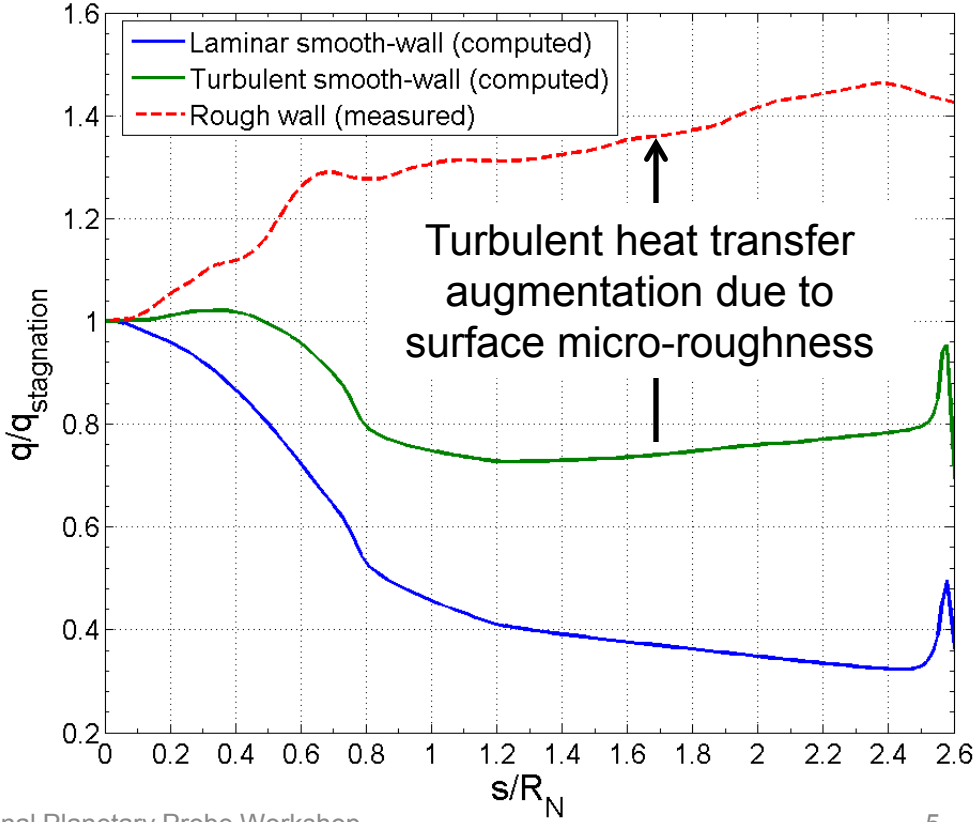

Statement of the Problem

- **For densely-packed roughness elements (sand grain roughness), the heating augmentation factor correlates with the roughness Reynolds number, which is proportional to the ratio of the roughness height to the viscous sublayer thickness**

$$\mathbf{Re_k^* = \rho_w U_\tau / \mu_w \propto \bar{k}/\delta_s}$$

where ρ_w, μ_w are the fluid density and viscosity at the wall,

$U_\tau = (\tau_w/\rho_w)^{1/2}$ is the smooth-wall friction velocity,

τ_w is the surface shear stress,

δ_s is the sublayer thickness, and

$\bar{k}$ is the mean roughness height

Statement of the Problem

Ablation under turbulent flow conditions can form macro-roughness patterns (not considered in current tests)

- These result from fluid-material interactions and form complex patterns not easily characterized by a single parameter like $\bar{k}$
- Macro-roughness affects heating mainly through changes in the inviscid flow rather than through changes in the boundary layer

Example Patterns formed on

Wind Tunnel Model

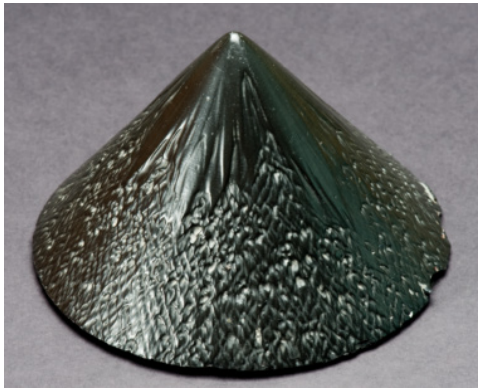

Ballistic Range Model

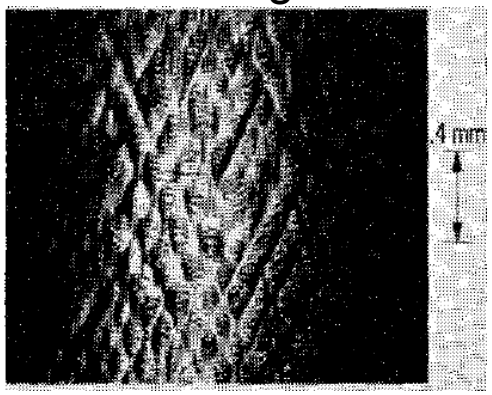

Objectives of the Experiments

- **Obtain data set of turbulent heat-transfer augmentation due to surface micro-roughness:**
  - 45° sphere-cone representative of Outer Planet probe geometry (nose radius = ½ base radius)
  - Test conditions selected to produce smooth-wall turbulent heating rates representative of an atmospheric entry at Saturn or Uranus (stagnation heat flux of 0.5 - 3 kW/cm^2)
  - Initial tests conducted in air in order to allow comparison with existing wind-tunnel data
- **Relate results to computed flight conditions**

Experimental Approach

Experiments were conducted in the Hypervelocity Free Flight Aerodynamic Facility at NASA Ames Research Center

- 23 m long enclosed flight range with 16 optical measurement stations
- Provides the capablility of testing in different atmospheres: Air, N_2, CO_2, Ar, H_2/He, and other gases
- Test-section pressures from 1 atm to ~0.0001 atm
- Capable of testing at speeds up to ~8 km/s
  - Top speed depends on choice of model launcher and projectile mass
  - Largest hypervelocity model launcher diameter = 3.8 cm

Ballistic Range Facility

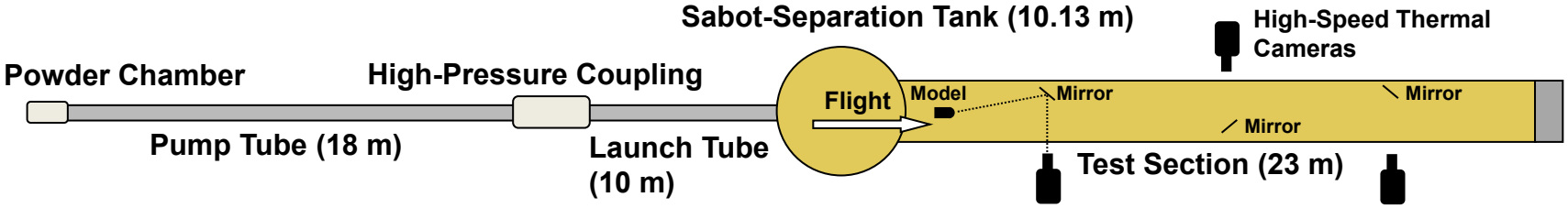

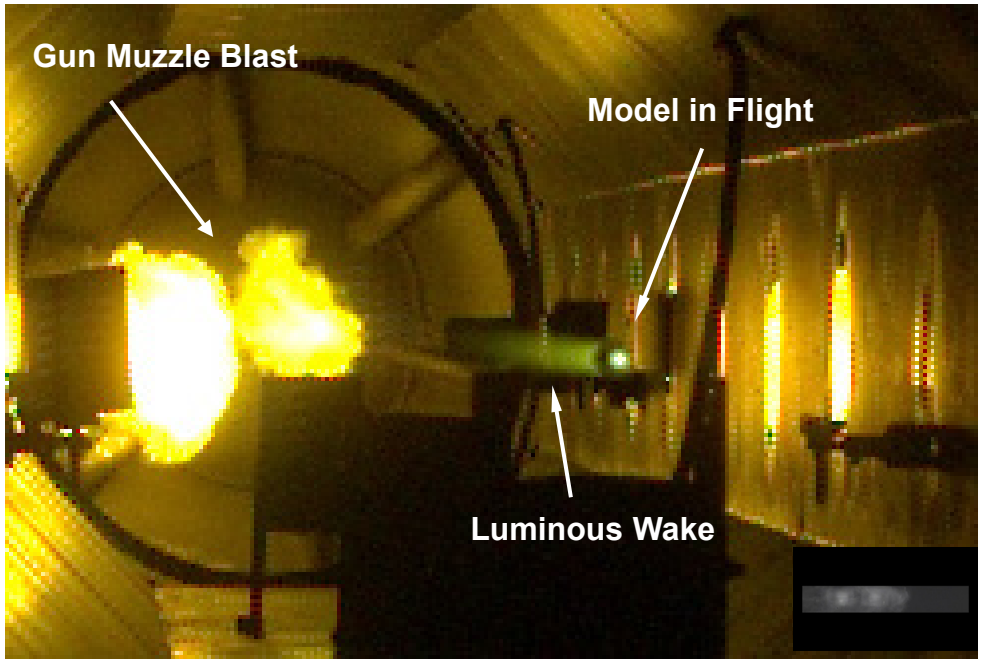

Capability to Independently vary P_∞,V_∞, and test gas

Experimental Approach

- **Test conditions selected to produce smooth-wall convective heating rates representative of atmospheric entry to Saturn or Uranus**
- **Air selected as test gas**
  - To allow validation of test methodology against available data
- **Surface micro-roughness produced by grit blasting**
  - Roughness size controlled by grit-size selection
- **Models fabricated of non-ablating materials to ensure surface roughness character did not change during flight**
  - Titanium or stainless steel

Ballistic Range Models

Typical Probe Geometry
45° Sphere-Cone

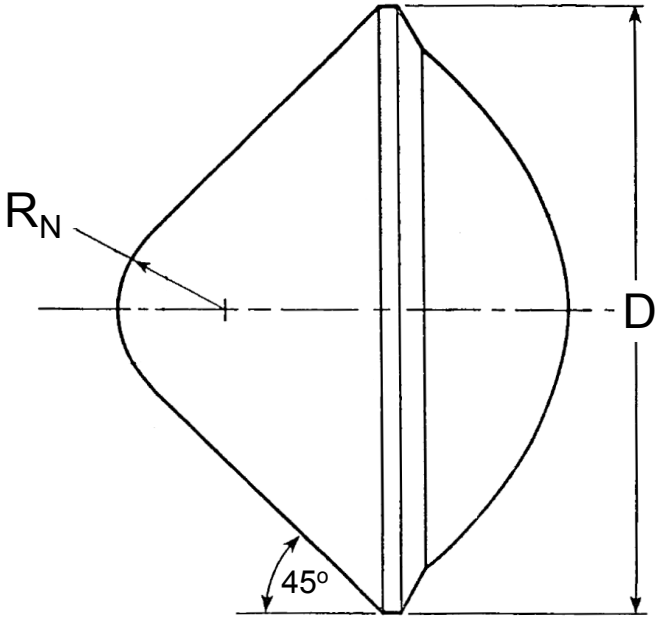

Saturn Probe: R_N = 0.25 m, D = 1 m
Uranus Probe: R_N = 0.19 m, D = 0.76 m

Ballistic Range Model in Flight
45° Sphere-Cone Forebody

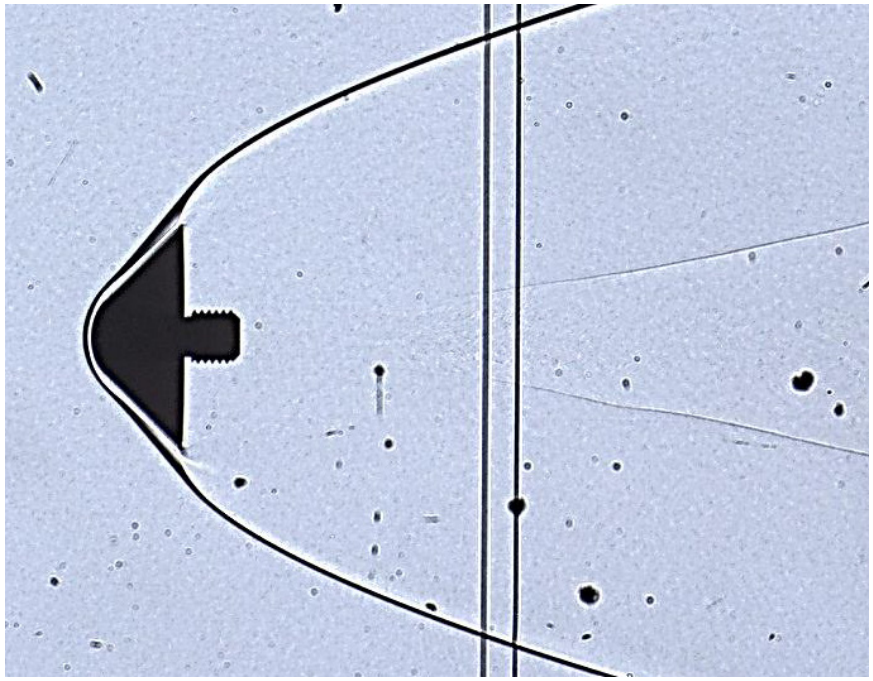

R_N = 0.762 cm, D = 3.3 cm
R_N = 3% Saturn Probe R_N
R_N = 4% Uranus Probe R_N

Set of Ballistic Range Models

Mean roughness height on each conic frustum:

$\bar{k}$ = 1.0 μm 4.8 μm 7.8 μm 13.9 μm 17.4 μm 22.8 μm

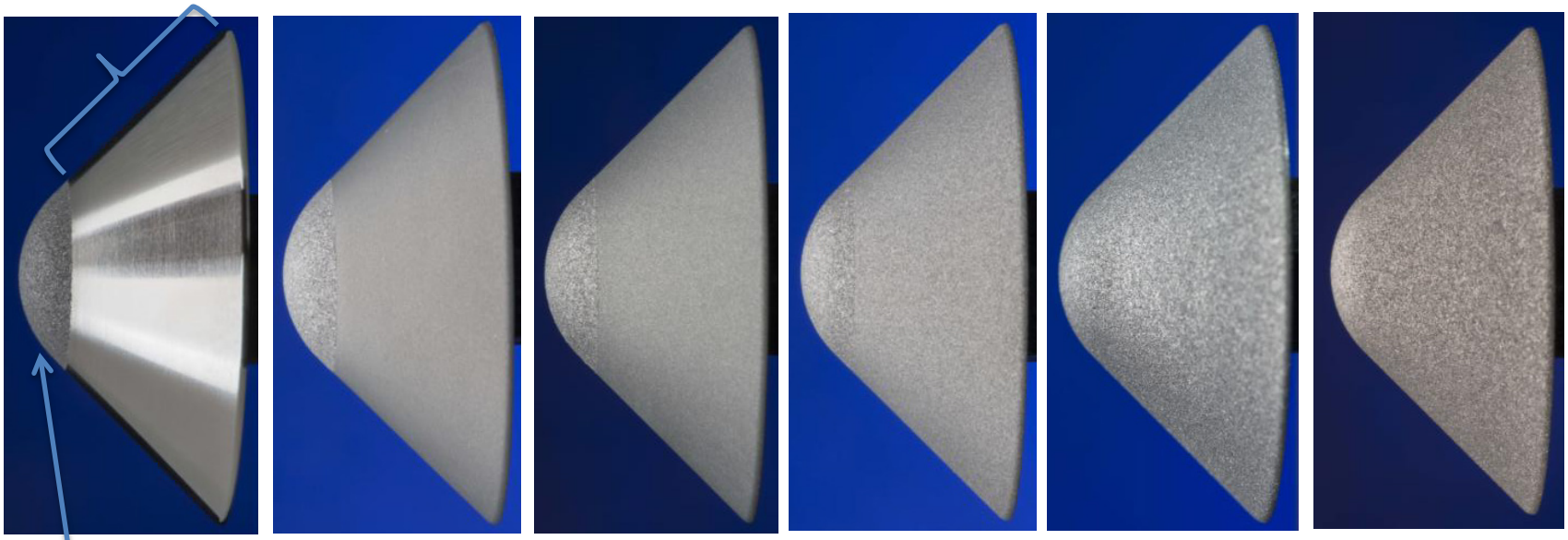

$\bar{k}_N \approx 16$ μm

Distributed roughness on each nosecap used to trip the flow, extended to sphere-cone tangent point, $s/R_N = 0.78$

Roughness Characterization

Each roughness distribution was measured using 3D non-contact profilometry (white-light interferometry)

Cone $\bar{k}$ = 4.8 μm
Nose $\bar{k}_N$ = 16 μm

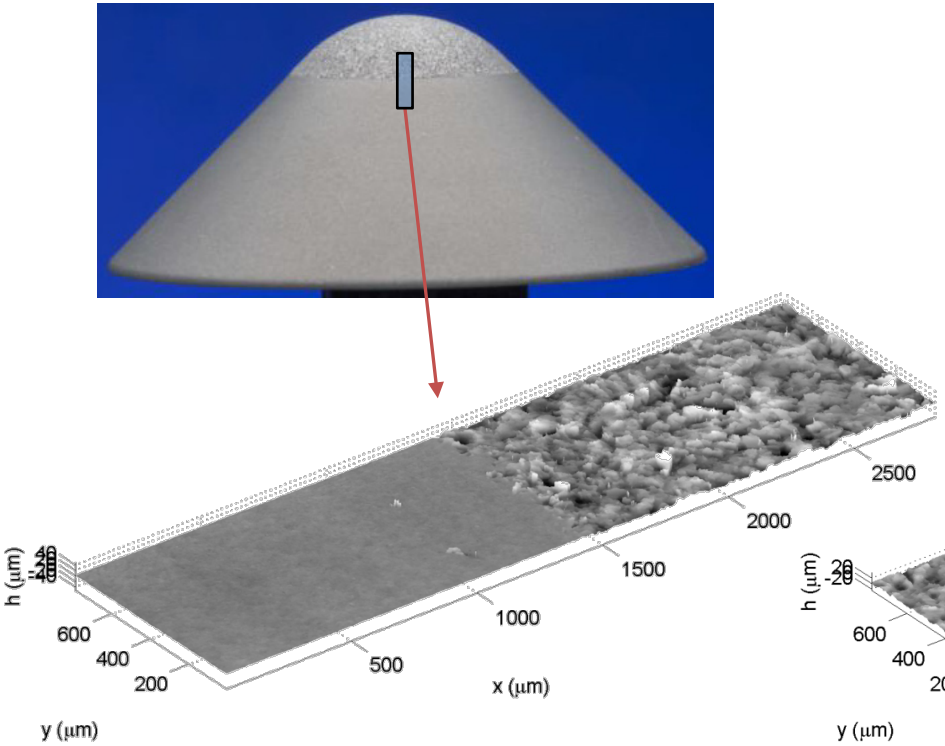

Cone $\bar{k}$ = 17.4 μm
Nose $\bar{k}_N$ = 15 μm

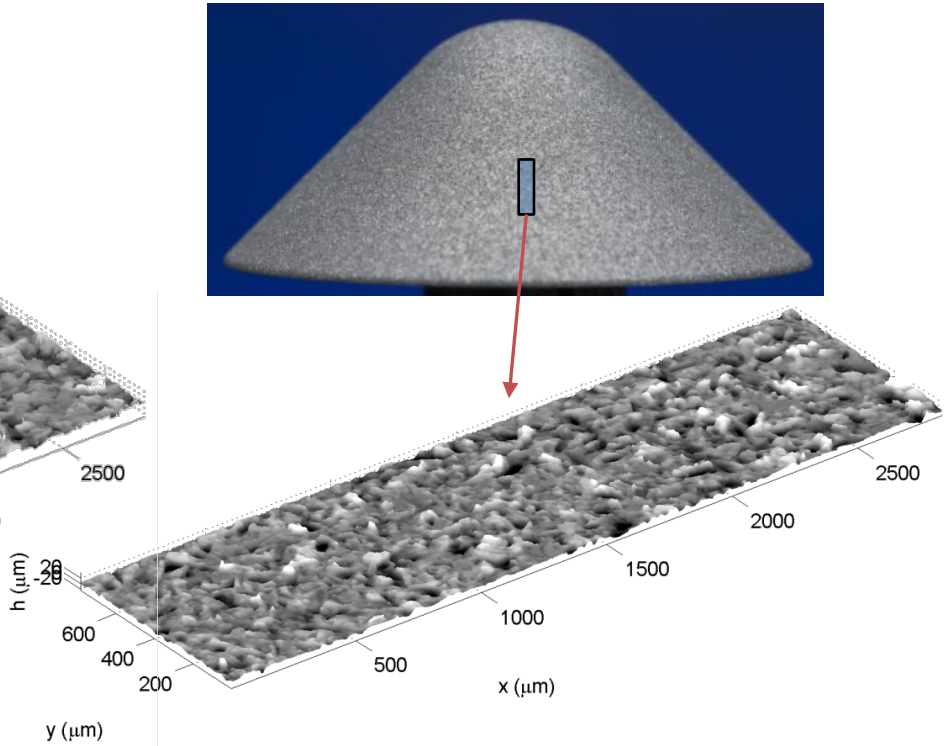

Roughness Characterization

- **Surface roughness maps topographically analyzed**
- **Roughness distributions characterized by mean peak-to-valley height, $\bar{k}$, of roughness elements**

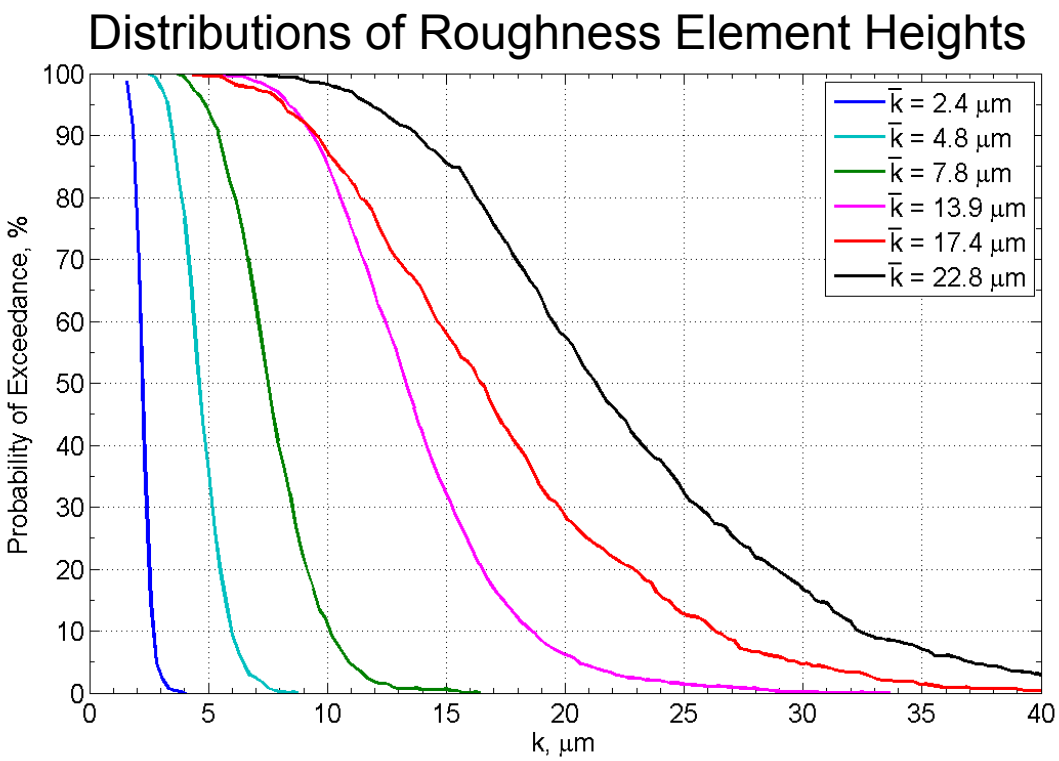

Experimental Approach

- **Each model of a set was flown at the same nominal conditions**
- **Convective heat flux measured in flight**
  - global surface temperature distributions captured at multiple points along the flight trajectory using high-speed infrared cameras
- **Heat-flux augmentation factor, q_r/q_s, determined**
  - q_s = smooth-wall turbulent convective heat flux
  - q_r = rough-wall turbulent convective heat flux
- **Roughness Reynolds number, Re_k^*, determined for each test from measured $\bar{k}$ and computed boundary-layer properties**

Thermal Imaging Example

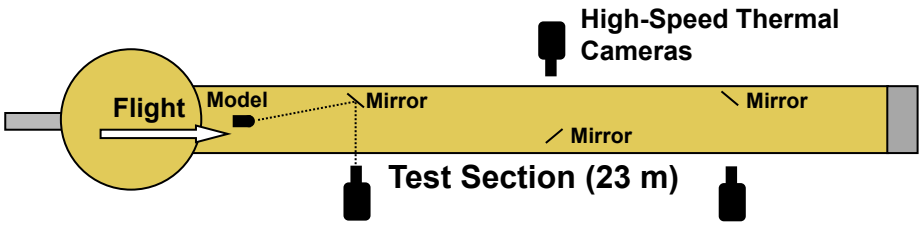

Infrared Image of Model in Flight

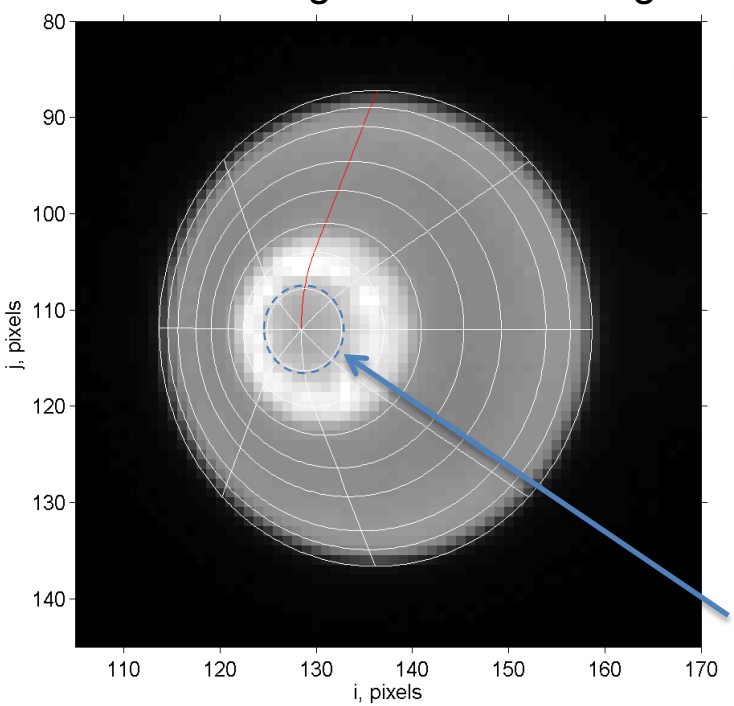

Convert IR intensity to Temperature, Map to Surface Grid

Surface Temperature Distribution

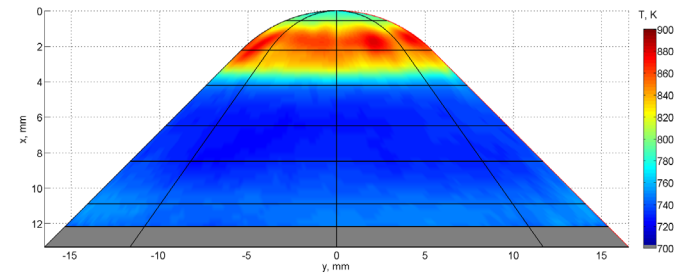

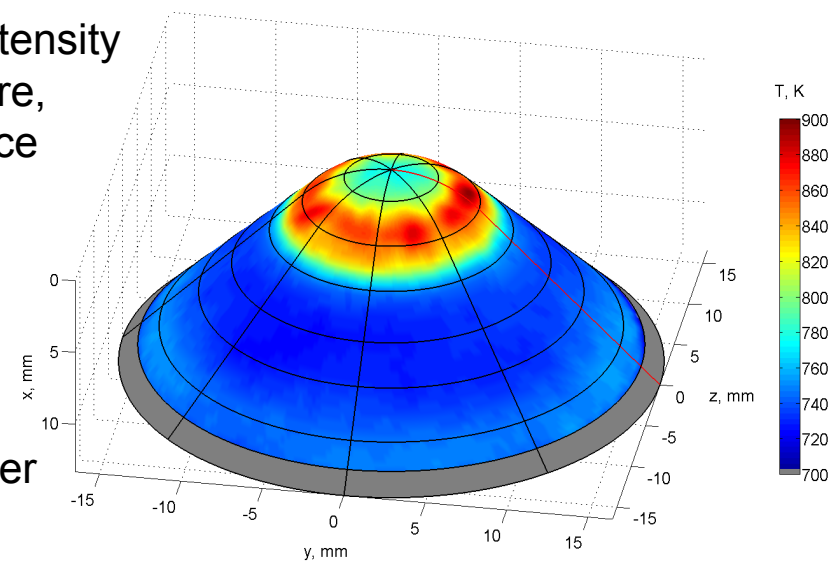

Boundary-layer Transition Front

Example Heat Flux Profiles

Each Image averaged circumferentially to give mean profile

Boundary Layer Transition Location on Rough Nosecaps

All Smooth

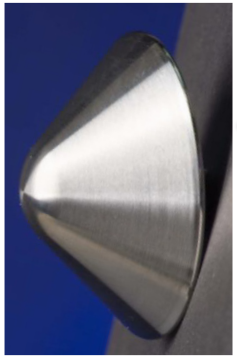

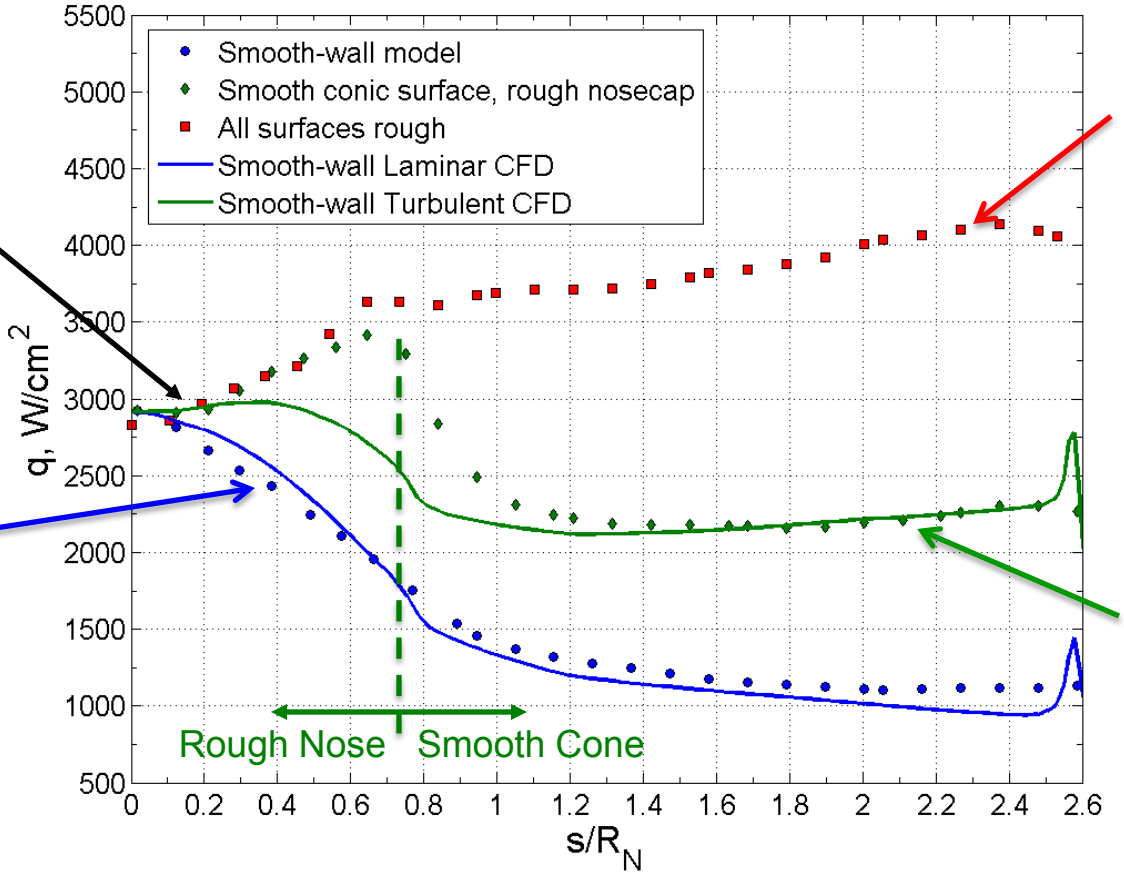

All Rough

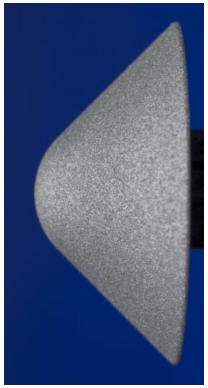

Smooth Cone Rough Nose

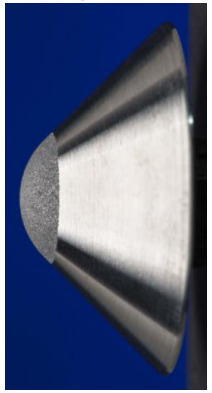

Results: Global Heat Flux Distributions

V_∞ = 3 km/s (M_∞ = 8.5), P_∞ = 0.15 atm (air)
δ_s = 2.8 μm

Mean roughness height on each conic frustum:

$\bar{k}$ =	2.4 μm	4.8 μm	7.8 μm	13.9 μm	17.4 μm	22.8 μm
$\bar{k}/\delta_s$ =	0.8	1.7	2.8	4.9	6.1	8.1
Re_k^* =	9	19	30	54	68	89

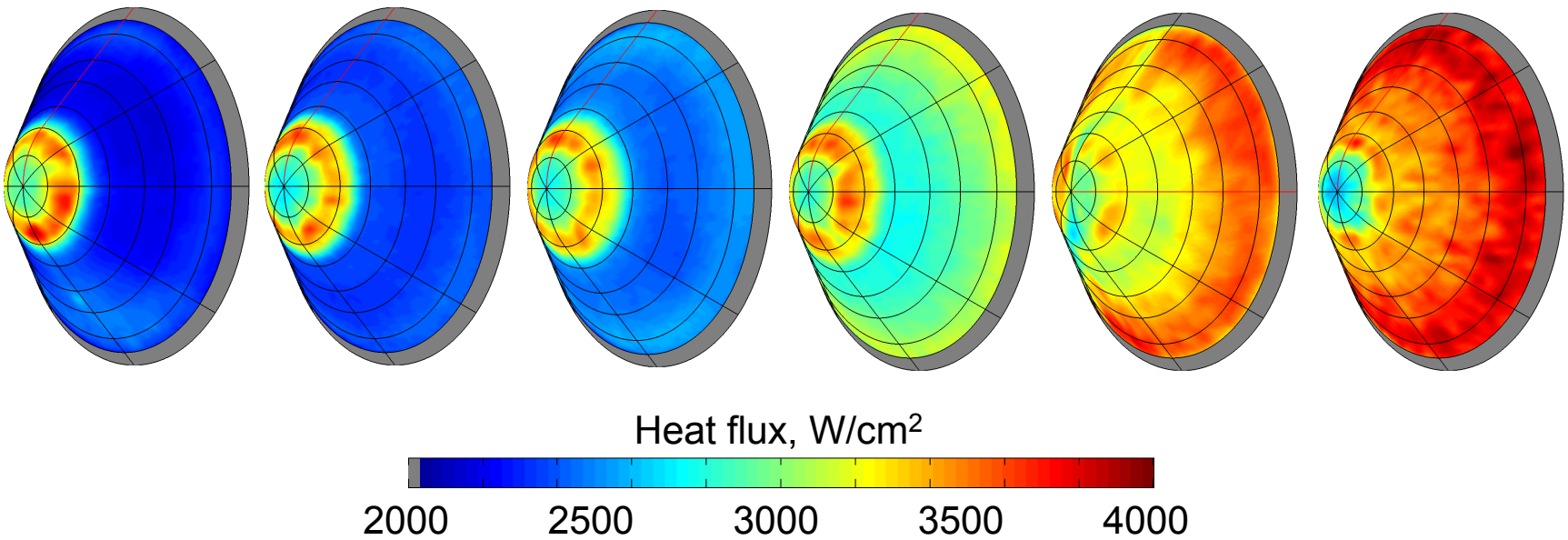

Results: Mean Heat Flux Profiles

V_∞ = 3 km/s (M_∞ = 8.5), P_∞ = 0.15 atm (air)

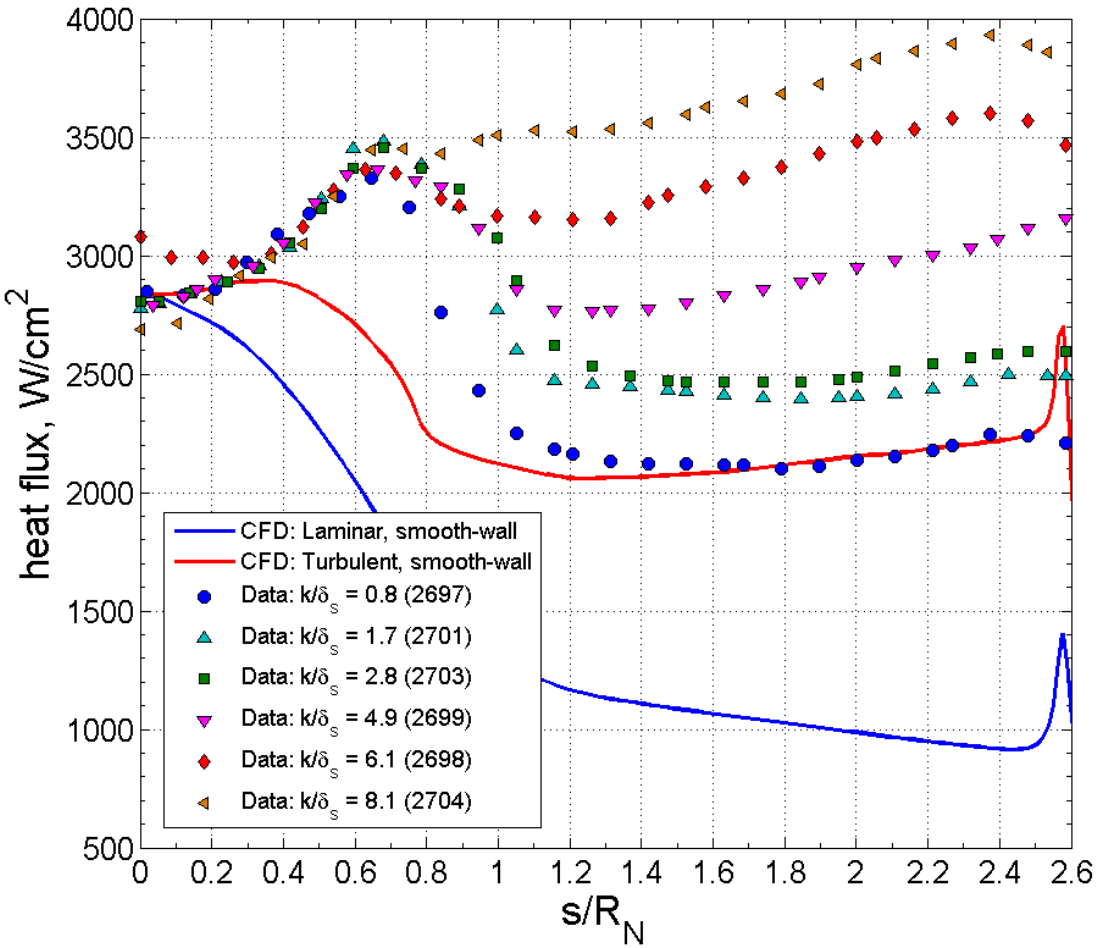

Increasing Roughness Size

Smooth Cone, $s/R_N > 0.78$

Results: Mean Heat Flux Profiles

V_∞ = 3 km/s (M_∞ = 8.5), P_∞ = 0.15 atm (air)

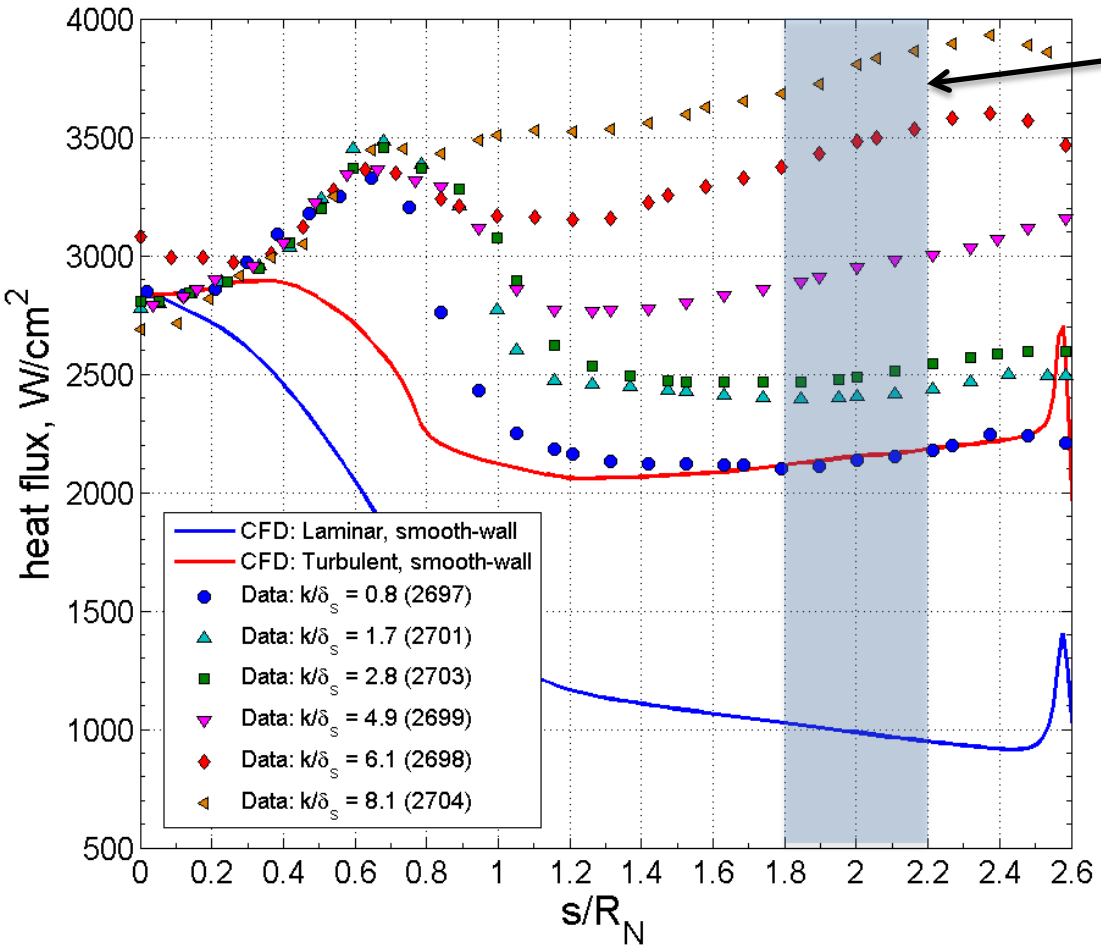

For each profile, heat flux is averaged over a span of the conic surface $1.8 < s/R_N < 2.2$ and the ratio of rough- to smooth-wall heat flux, q_r/q_s, is formed

- s/R_N = 1.8 is sufficiently far downstream of the nose roughness (trip) to form a turbulent boundary layer profile
- s/R_N = 2.2 is sufficiently far upstream to avoid potential interference from the launch sabot

Results: Heating Augmentation Factor

Heating augmentation factors on 45° sphere-cone

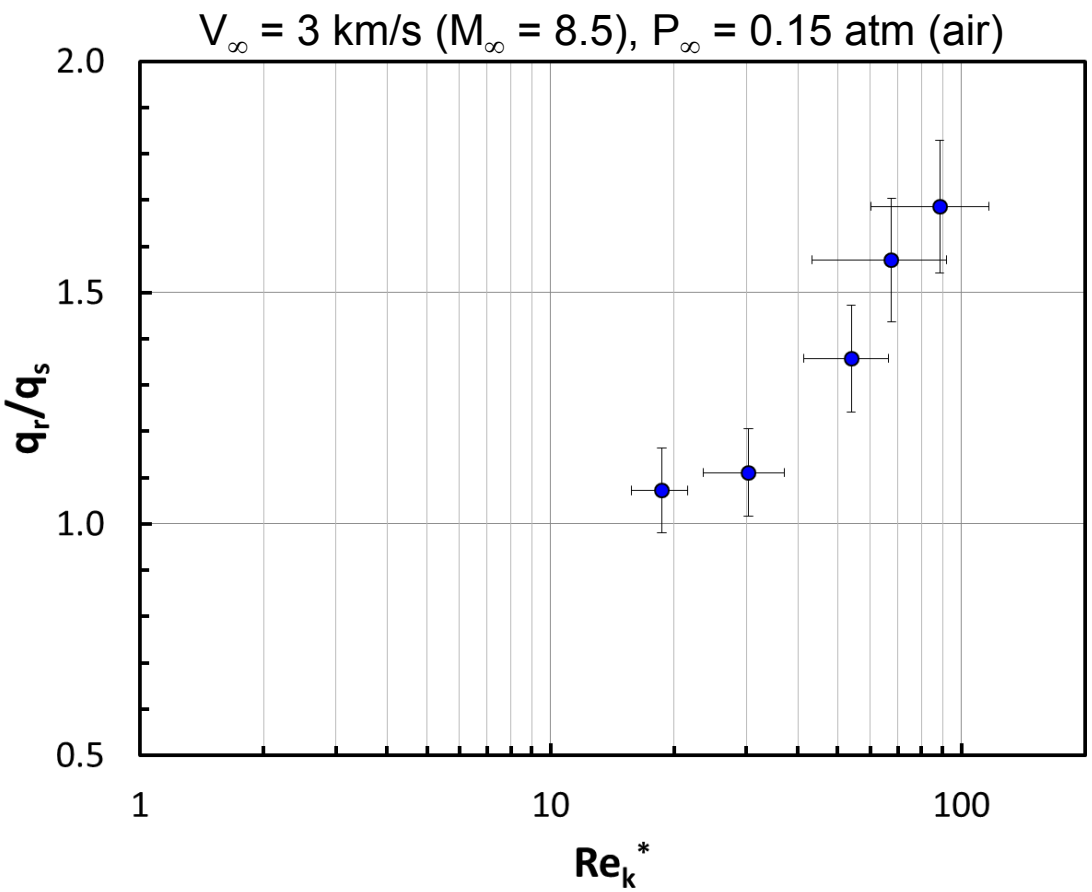

Results: Heating Augmentation Factor

Results have been obtained at three test conditions:

V_∞, km/s	2.5	3.0	3.4
Re_D	0.5 x10^6	0.9 x10^6	2 x 10^6
M_∞	7.5	8.5	10
q_s, W/cm^2	930	2100	3300
P_{stag}, atm	8	16	38
δ_s, mm	3.36	2.8	1.9
Cone angle	45°	45°	30°

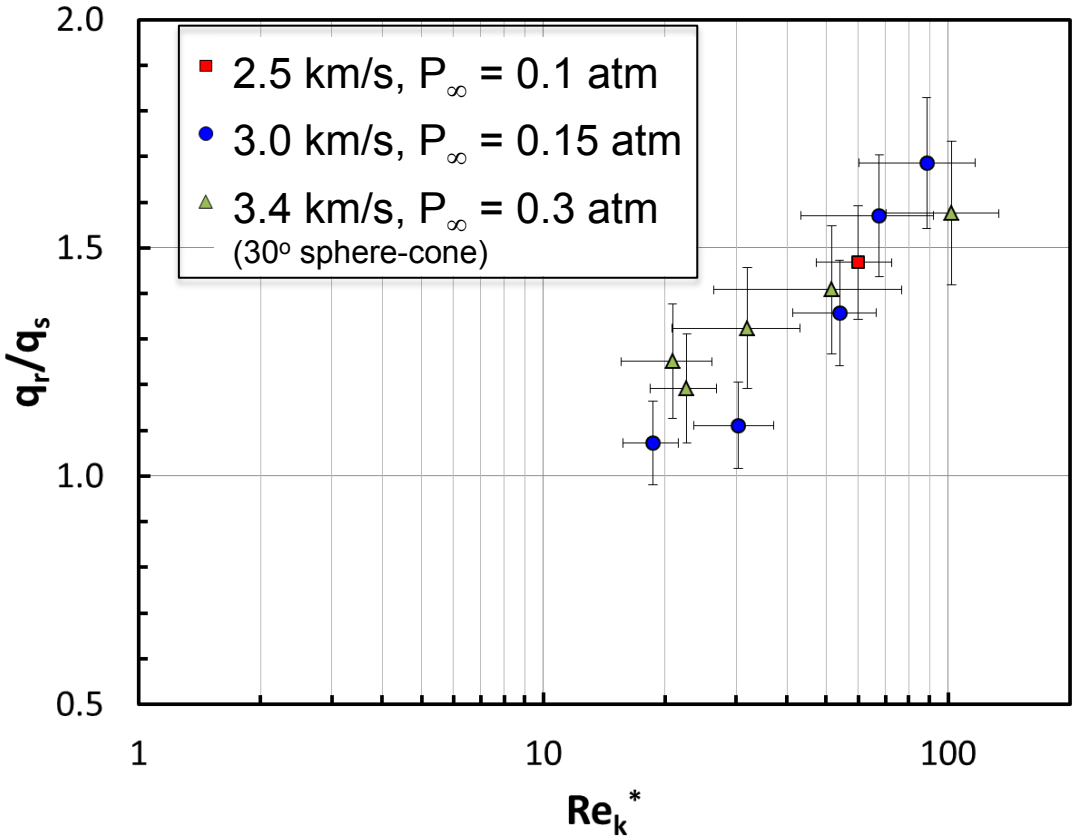

Results: Heating Augmentation Factor

Comparison with Data from the PANT Program (Passive Nosetip Technology)[1]

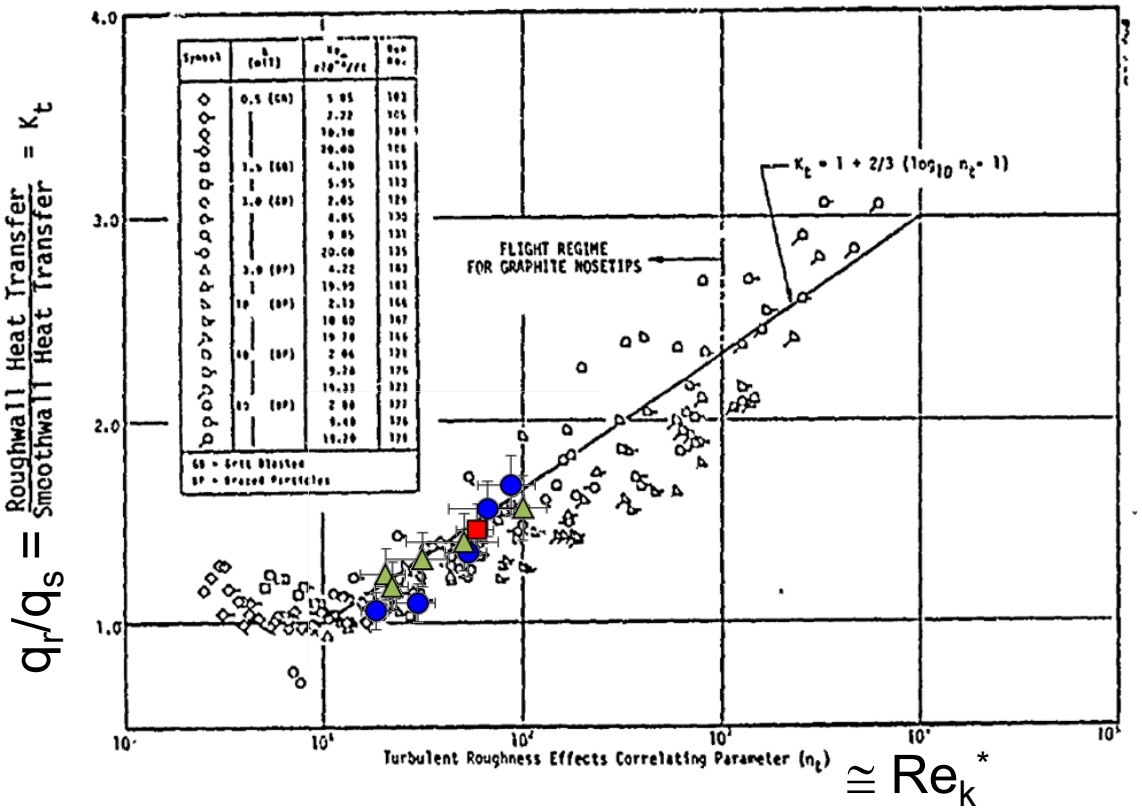

Nosetip Model

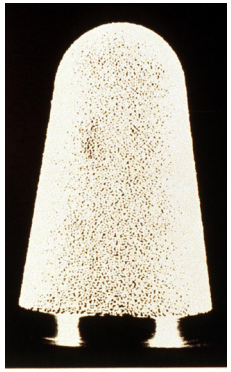

[1]Wool, M. R., "Final Summary Report Passive Nosetip Technology (PANT) Program," Aerotherm Report 75-159, June 1975.

Results: Implications for Flight

- **Entry Trajectories were derived based on 2013-2023 Planetary Science Decadal Survey**
- **Heat flux and boundary-layer parameters computed at peak convective heating[1]**
- **Boundary-layer viscous sublayer thickness determined**

	Saturn 216 kg probe	Uranus 127 kg probe
Re_D	0.26×10^6	11×10^6
Mach #	18	15
Stagnation pressure, atm	0.3	9
Stagnation q_0, W/cm^2	785	1760
Mid-frustum q_s, W/cm^2	614	1550
δ_s, mm	**1.08**	**0.12**

[1]Palmer, et al., "Uncertainty Determination for Aeroheating in Uranus and Saturn Probe Entries by the Monte Carlo Method," AIAA Thermophysics Conference, June, 2013.

Results: Implications for Flight

Saturn entry trajectory:

- A roughness > 1 mm is required for the onset of roughness augmentation of turbulent heating due to the thick boundary layer (δ_s ~ 1 mm)

Uranus entry trajectory:

- Augmentation factors as high as 70% possible for roughness of 1 mm

Re_k^* for 0.1 mm < $\bar{k}$ < 1 mm
Uranus entry trajectory

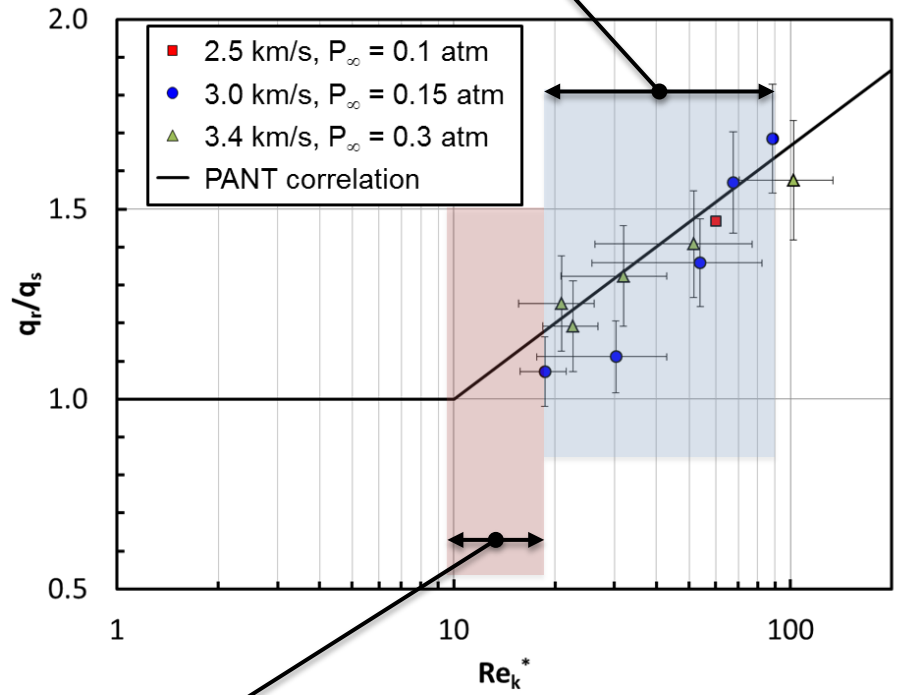

Re_k^* for 1 mm < $\bar{k}$ < 10 mm
Saturn entry trajectory

Summary

- **Data were obtained to quantify turbulent heat-transfer augmentation due to surface roughness on an Outer Planet probe geometry in hypersonic free flight**
  - Test conditions span a range of convective heat transfer rates representative of Outer Planet entry environments
  - Results validated against wind-tunnel data obtained on other configurations
- **Augmentation factors up to 70% possible for roughness of 1 mm for Uranus entry trajectory, when considering roughness alone.**

Future work

- **Complete current test series**
- **Employ ballistic range capability to test in various gases to expand data set to other atmospheres**
  - Aerodynamic coefficients, such as drag, have been shown to differ in gases with different specific heat ratios[1,2]

[1]Intrieri, P. F., and De Rose, C. E., "Flight Characteristics of Probes in the Atmospheres of Mars, Venus and the Outer Planets," *Acta Astronautica*, Vol. 4, 1977.

[2]Brown, J., et al., "Free Flight Testing in Support of the Mars Science Laboratory Aerodynamics Database," *Journal of Spacecraft and Rockets*, Vol. 43, No. 2, 2006.